



# Supernova Remnant Evolution in Wind Bubbles: A Closer Look at Kes 27

V. V. Dwarkadas<sup>a</sup>, D. Dewey<sup>b</sup>

<sup>a</sup>Department of Astronomy and Astrophysics, University of Chicago, TAAC 55, Chicago, IL 60637

<sup>b</sup>MIT Kavli Institute, Cambridge MA 02139

---

## Abstract

Massive Stars ( $> 8M_{\odot}$ ) lose mass in the form of strong winds. These winds accumulate around the star, forming wind-blown bubbles. When the star explodes as a supernova (SN), the resulting shock wave expands within this wind-blown bubble, rather than the interstellar medium. The properties of the resulting remnant, its dynamics and kinematics, the morphology, and the resulting evolution, are shaped by the structure and properties of the wind-blown bubble. In this article we focus on Kes 27, a supernova remnant (SNR) that has been proposed by [1] to be evolving in a wind-blown bubble, explore its properties, and investigate whether the properties could be ascribed to evolution of a SNR in a wind-blown bubble. Our initial model does not support this conclusion, due to the fact that the reflected shock is expanding into much lower densities.

© 2011 Published by Elsevier Ltd.

### Keywords:

Hydrodynamics, Shock waves, Stars: massive, Stars: winds, outflows, ISM: bubbles, ISM: supernova remnants

---

## 1. Introduction

About 80% of supernovae (SNe) arise from the core collapse of massive stars. These stars experience strong mass-loss in the form of winds, modifying the medium around them and creating low density wind blown bubbles surrounded by dense shells [25, 24, see also Dwarkadas & Rosenberg HEDLA 2012 proceedings]. When the supernova remnant (SNR) shock interacts with the dense shell, it results in a transmitted shock that expands slowly into the denser medium, and a reflected shock that initially travels back into the already-shocked lower-density medium. The reflected shock continues to travel inward and eventually passes the reverse shock, speeding its progress into the SN ejecta.

The kinematic and morphological properties of the SNR would be determined by its expansion in the bubble [9]. Expansion of a SNR in a wind bubble has been studied by many authors [4, 23, 22, 14, 13, 12]. One of the most famous examples of a SNR expanding in a pre-existing wind-blown cavity is the nearby SN 1987A, which has been extensively studied [3, 19, 11, 6]. Although many, if not most, core-collapse SNe should be evolving in wind-blown cavities, it is difficult to find many clear observational examples, and therefore to compare the theoretical models to observations. In this paper we wish to study the SNR Kesteven 27, which has been suggested as being an example of a SNR in a wind-blown cavity.

---

Email addresses: [vikram@oddjob.uchicago.edu](mailto:vikram@oddjob.uchicago.edu) (V. V. Dwarkadas), [dd@space.mit.edu](mailto:dd@space.mit.edu) (D. Dewey)

## 2. Kes 27

Kesteven 27 is a member of the class of thermal composite or mixed-morphology remnants [20], which show thermal X-ray emission extending a long way in to the center. X-ray data has been obtained using *Einstein*, *ROSAT*, *ASCA* and *Chandra*. In the radio band it has been observed at 843 MHz with *MOST* [26]. The radio emission is brightest towards the East, but fades towards the Northwest. The *Chandra* image (Fig 1, [1]) show two incomplete shell-like features in the northeastern half, with brightness fading towards the southwest. The X-ray and radio structure led Chen et al. 2008 [1, hereafter CSSL08] to suggest that the morphology represents a SNR expanding in a wind-blown bubble, as shown in Fig 1. In their view, the remnant is colliding with an HI shell to the northeast, sending a reflected shock back into the interior. The two circular arcs were assumed to be representative of emission from near the location of transmitted and reflected shock waves. Calculations based on equations by [21] were used to quantify their claims.

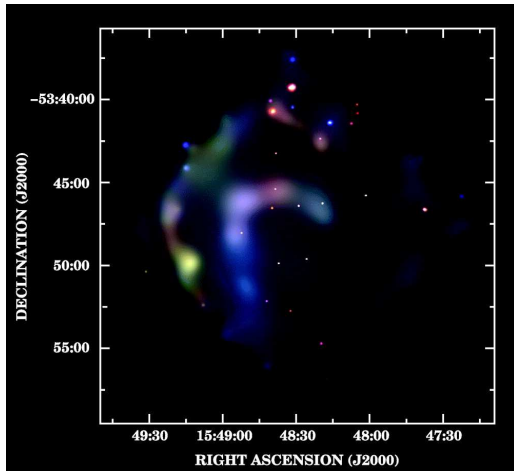


Figure 1. Tricolor ACIS-I image of Kes 27. Taken from [1], reproduced by permission of the AAS. The X-ray intensities in the 0.3-1.5, 1.5-2.2, and 2.2-7.0 keV bands are coded red, green, and blue, respectively, and are scaled logarithmically in the ranges 19-170, 19-290, and 27-270 photons  $\text{cm}^{-2} \text{s}^{-1} \text{sr}^{-1}$ .

## 3. Numerical Simulations

We have carried out numerical hydrodynamic simulations to understand the structure of Kesteven 27, with the intention of exploring the reflected shock model suggested by [1]. The simulations were carried out using the VH-1 finite difference hydrodynamic code in 2D spherical co-ordinates. Radiative cooling was included via a cooling function. Further details of the numerical method are described in earlier papers [16, 14, 12]

Our basic model has the following parameters: A power-law ejecta density structure as defined in [5], with ejecta density assumed to decrease as  $r^{-9}$  [2], and an ejecta mass of  $4.5 M_{\odot}$ . The shock first expands into a low density medium ( $n_H=0.1$ ), stretching for about 8.4 pc, then collides with a higher density HI shell, with  $n_H = 0.5$ . In Fig 2, we show density snapshots from the evolution. Time in years is given at the top of each plot. Initially (Fig 2, top row), the expansion of the SN ejecta into the medium gives rise to a forward shock expanding into the medium and a reverse shock going back into the ejecta, separated by a contact discontinuity. As the shock expands into the low density medium, the decelerating contact discontinuity is seen to become Rayleigh-Taylor unstable, as expected [15]. After about 1500 years, the forward shock collides with the denser HI shell, giving rise to a slowly expanding shock transmitted into the HI shell, and a faster moving reflected shock that moves much faster through the low density interior (Fig 2, bottom row). At about 3500 years the radii of the transmitted and reflected shocks are approximately consistent with the positions of the observed arcs. Thus our models are able to reproduce the gross morphology suggested by CSSL08.

To explore whether the X-ray morphology and emission is consistent with the observations, we have made preliminary calculations of these quantities from the simulations. Averaging over radial profiles, we have extracted mean radial profiles of density and temperature from the 2D simulations. The temperature is used to compute the radial X-ray emissivity (flux per density-squared) by evaluating a simple non-equilibrium X-ray emission model (`vnei`) with  $T_e = 0.2 T_{\text{hydro}}$ ,  $n_{\text{et}} = 3 \times 10^{11} \text{ cm}^{-3}$ , and abundances determined from the X-ray data. Using the ISIS [17] and V3D [7] packages, we convert the radial values into simulated 3D images for several quantities from the last timestep. We find that, unlike the observed data, the simulated X-ray image (Fig 3, right image) in this case shows only one outer ring of emission and does not show any inner arc coincident with the reflected shock. Although hot X-ray emitting gas is certainly present at the inner locations (Fig 2 middle image), the reason this inner ring is not visible is that the inner shock is traveling into a much lower density region (Fig 2 left image). Since X-ray emissivity is proportional to the square of the density, the  $\geq 5$  times lower density results in a decrease in X-ray flux by a factor of over 25, and thus no appreciable amount of emission is produced in the interior.

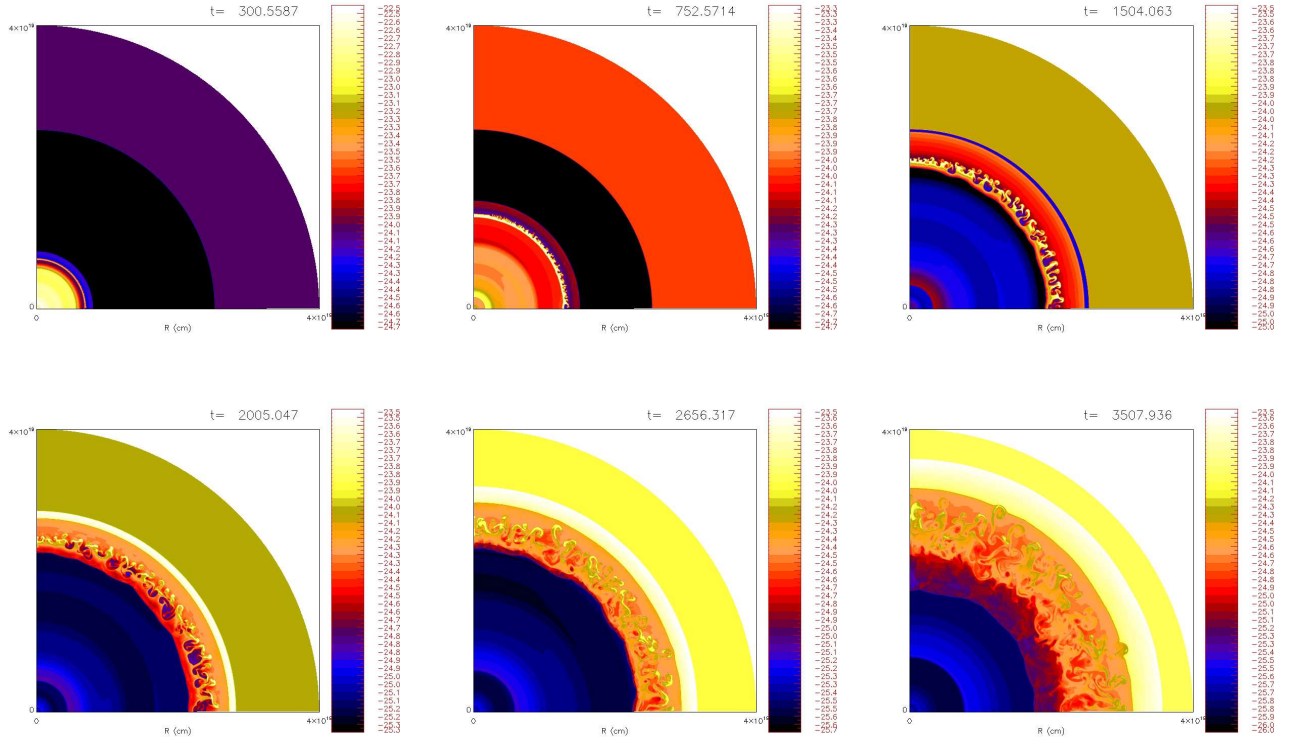


Figure 2. (1) Evolution of the SNR shock waves in a low density medium (2) Growth of Rayleigh-Taylor (R-T) instabilities is visible at the decelerating contact discontinuity. (3) The instabilities have grown in size as the forward shock approaches the HI shell. (4) Collision with the denser HI shell drives a slow-moving shock into the shell, and gives rise to a reflected shock moving back into the ejecta. (5) Transmitted and reflected shocks advance, while the R-T unstable region continues to grow. As the forward shock has slowed down considerably, the instabilities reach almost to the forward shock, which would not normally be the case. (6) Reflected and transmitted shocks have radii consistent with observations. However, as we show in the paper, emission from the reflected shock is very low compared to that from the forward shocked region.

#### 4. Discussion

As shown in the above simulations, we conclude that using the parameters generally defined in CSSL08, it is difficult to reproduce the observed X-ray morphology of Kes 27.

Is it likely that a different set of parameters would work? It seems unlikely in general as long as the reflected shock is traveling into the low density ejecta. In our simulations the reflected shock is already expanding into the constant

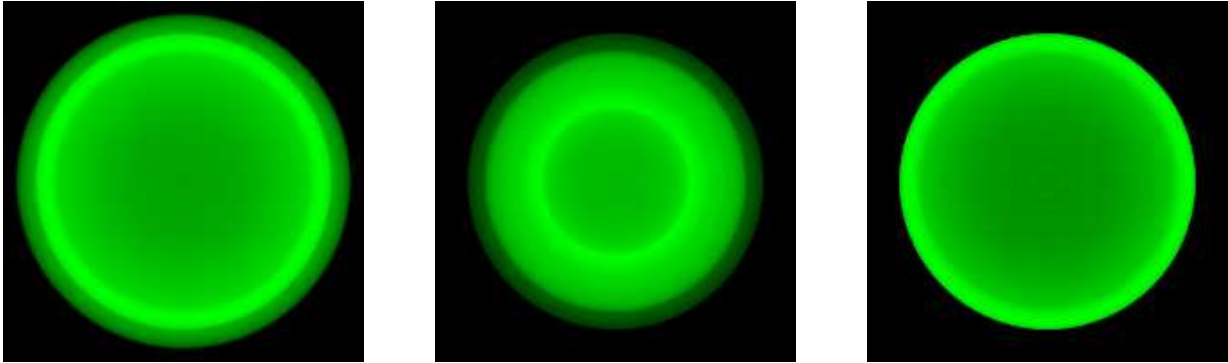


Figure 3. Simulated images based on the hydrodynamics. The radial average properties were used to make 3D images (using ISIS/V3D) assuming full spherical emission; the intensity scale is non-linear to better show the full range. The images correspond to the density (left), the X-ray emissivity for constant density (middle), and, finally, the X-ray emission taking into account the density-squared dependence (right). As can be seen, in projection only the outer ring is manifest, and hardly any emission is seen in the inner regions. The visualization does not produce two visible arcs as seen in Fig 1.

density plateau of the ejecta. While it may be supposed that the emissivity could be higher if it were still expanding in the steep power-law part of the ejecta density, it is unlikely that this would work in practice for a remnant that is a few thousand years old. This is because the ejecta density decreases with time as  $t^{-3}$ , and therefore no matter which part of the density profile it was interacting with, it would have decreased to a low value in about 3500 years. If the collision happened much earlier in the SNR history, and the ejecta mass was significantly larger, then it is possible that the parameters could be fine-tuned so that the reflected shock would be expanding in a high-enough density regime to provide appreciable emission.

But overall this appears unlikely. The model requires that the SNR collide with a high density shell in order to produce a reflected shock in the first place. This means that the density of the material into which the forward shock expands must by necessity be larger than that of the plasma in which the reflected shock is expanding. It is then difficult to come up with a set of conditions where the reflected shock finds itself in a region where the density is high enough to provide emissivity comparable to that of the forward shock. It is possible that a high metallicity in the low density region could raise the emissivity, and a really high density in the ambient medium could slow the forward shock down to the extent that its temperature, and therefore X-ray emissivity, is quite low. However these are extremes that do not easily fit into the scenario suggested by CSSL08, and it would be extremely difficult to produce a viable model with these characteristics.

It is hard to think of circumstances where the reverse shock is expanding into a denser medium than the forward shock is. One case that we have recently examined [10], for the very young SN 1996cr, may be able to provide some inspiration. This SN appears to have interacted with a dense shell of gas very early (a couple of years) after explosion. After about 7 years, the SN shock has crossed the dense shell and is expanding in a lower density medium, whereas the reverse shock is still in the higher density shell. The emission predominantly then arises from a reverse shock. If such a situation could be envisaged for an older SNR, where the forward shock has crossed a dense shell and is expanding in lower density material, whereas the reverse shock is still expanding in the higher density material, then it is possible that we could reproduce two arcs of emission.

In future we will carry out a more thorough parameter survey to study the remnant expansion, keeping the above factors in mind. We also plan improvements to our techniques to allow us to use the full multi-dimensional simulations in calculations of the X-ray emission, and production of simulated images.

#### 4.1. Relation to High Energy Physics Lab Experiments

In keeping with the theme of lab astrophysics at this conference, we suggest that this is an astrophysical scenario that is quite feasible to be carried out with available apparatus [8, 18], and thus to be studied under controlled settings in the laboratory. Basically one needs to create an environment which is partially filled with medium 1 of a given density, and partly with medium 2 that has density 5 times higher. A strong shock expands first in medium 1, and then collides with medium 2, which has the higher density. The collision would lead to the formation of a transmitted and reflected

shock at the interface. The structure and expansion of these shocks must be studied over a few doubling times. All shocks would be non-radiative. This would allow a very interesting and potentially significant astrophysical scenario to be studied in the laboratory, which could answer pertinent questions about shock propagation in wind bubbles and other astrophysical environments.

## 5. Acknowledgments

VVD's research is funded by grant TM1-12005X, provided by NASA through the Chandra X-ray Observatory center (CXC), operated by SAO under NASA contract NAS8-03060. DD's research is supported by SAO contract SV3-73016 to MIT for support of the CXC and Science Instruments.

## References

- [1] Chen, Y., Seward, F. D., Sun, M., & Li, J.-t. 2008, *ApJ*, 676, 1040
- [2] Chevalier, R. A., & Fransson, C. 1994, *ApJ*, 420, 268
- [3] Chevalier, R. A., & Dwarkadas, V. V. 1995, *ApJL*, 452, L45
- [4] Chevalier, R. A., & Liang, E. P. 1989, *ApJ*, 344, 332
- [5] Chevalier, R. A. 1982, *ApJ*, 258, 790
- [6] Dewey, D., Dwarkadas, V. V., Haberl, F., Sturm, R., & Canizares, C. R. 2012, *ApJ*, 752, 103
- [7] Dewey, D., & Noble, M. S. 2009, *Astronomical Data Analysis Software and Systems XVIII*, 411, 234
- [8] Drake, R. P., Smith, T. B., Carroll, J. J., III, et al. 2000, *ApJS*, 127, 305
- [9] Dwarkadas, V. V. 2011, *MMSal*, 82, 781
- [10] Dwarkadas, V. V., Dewey, D., & Bauer, F. 2010, *MNRAS*, 407, 812
- [11] Dwarkadas, V. V. 2007, *Supernova 1987A: 20 Years After: Supernovae and Gamma-Ray Bursters*, 937, 120
- [12] Dwarkadas, V. V. 2007, *ApJ*, 667, 226
- [13] Dwarkadas, V. V. 2007, *Revista Mexicana de Astronomia y Astrofisica Conference Series*, 30, 49
- [14] Dwarkadas, V. V. 2005, *ApJ*, 630, 892
- [15] Dwarkadas, V. V. 2000, *ApJ*, 541, 418
- [16] Dwarkadas, V. V., & Balick, B. 1998, *AJ*, 116, 829
- [17] Houck, J. C., & Denicola, L. A. 2000, *Astronomical Data Analysis Software and Systems IX*, 216, 591
- [18] Klein, R. I., Budil, K. S., Perry, T. S., & Bach, D. R. 2003, *ApJ*, 583, 245
- [19] McCray, R. 2007, *Supernova 1987A: 20 Years After: Supernovae and Gamma-Ray Bursters*, 937, 3
- [20] Rho, J., & Petre, R. 1998, *ApJL*, 503, L167
- [21] Sgro, A. G. 1975, *ApJ*, 197, 621
- [22] Tenorio-Tagle, G., Rozyczka, M., Franco, J., & Bodenheimer, P. 1991, *MNRAS*, 251, 318
- [23] Tenorio-Tagle, G., Bodenheimer, P., Franco, J., & Rozyczka, M. 1990, *MNRAS*, 244, 563
- [24] Toalá, J. A., & Arthur, S. J. 2011, *ApJ*, 737, 100
- [25] Weaver, R., McCray, R., Castor, J., Shapiro, P., & Moore, R. 1977, *ApJ*, 218, 377
- [26] Whiteoak, J. B. Z., & Green, A. J. 1996, *A&A Supp.*, 118, 329